



Vol. 3 No. 4 (April) (2025)

Photocatalytic and Photovoltaic properties of 2D Materials

Shehroz Abdullah

Ph.D Physics Research Scholar

Material Modeling Lab, Department of Physics, Islamia College University
Peshawar, KP Pakistan, 25120

Email: shehroz.abdullah0300@gmail.com

Dr. Ghulam Murtaza

Associate Professor

Material Modeling Lab, Department of Physics, Islamia College University
Peshawar, KP, Pakistan, 25120

Email: murtaza@icp.edu.pk

Muhammad Awais Jehangir

Material Modeling Lab, Department of Physics, Islamia College University
Peshawar, KP, Pakistan, 25120

Email: awaisislamian977@gmail.com

Abstract

The field of two-dimensional (2D) layered materials has made it possible to examine numerous physical phenomena that are interesting from a scientific perspective and relevant to technology applications on a new level. Innovative applications in electronics and energy storage leverage the distinct electrical, optical, and mechanical properties of two-dimensional materials to create indispensable components. Theoretical projections based on building on these advancements, these materials, which are atomically thin and have a high surface-to-volume ratio, are attractive for a range of applications, including hydrogen storage, sensing, batteries, and photo-catalysis. Atomically precise computer simulations of 2D materials are crucial for the development of novel materials. This paper mostly uses density functional theory and non-equilibrium Green's function to explore 2D materials. The electrical structure and transport characteristics are investigated for several synthetic and predicted 2D materials with different potential applications in electrodes for rechargeable batteries, gas sensors, and nanoscale electronic devices. Both horizontal and vertical heterostructures have been studied in order to apply lateral and vertical heterostructures in nanoscale devices, such as the twisted bilayer black phosphorus Nano junction, where electronic and transport properties were investigated for a device with diode-like properties, and the graphene/hBN heterostructure Nano gap for a potential DNA sequencing device. We also covered the structural, electrical, and transport properties of the recently discovered borophenes, which are polymorphs of 2D borons. We have looked into the conventional methods of modifying the properties of the material, such as strain in borophene and substitutional doping in black phosphorus, along with the potential applications for gas sensing. A sizable portion of this thesis is devoted to the applications of different 2D materials for energy storage. Rechargeable batteries with high energy and power densities are the goal of



Vol. 3 No. 4 (April) (2025)

energy storage technologies, which are crucial for providing effective ways to transfer and sell the energy generated. The simulation research contributes to knowledge while advancing the attributes. Among the elements that increase the batteries' efficacy.

Keywords. Density functional theory, Non-equilibrium Green's function, 2D materials, Energy storage, Electron transport

Introduction

It was long believed in the scientific community that two-dimensional (2D) materials might not truly exist (Butler, Hollen et al. 2013). Theorists in the early twentieth century predicted that the low-dimensional crystal would probably disintegrate at limited temperature because of the large lattice atom displacement caused by many sources of thermal fluctuations. It is frequently assumed that the magnitude of this displacement will be in the same order as the interatomic lengths of the material. More precisely, Mermin's research demonstrated that, as a thin film material's thickness falls, its melting point rapidly drops, a finding that is strongly supported by experimental evidence (Fischetti and Vandenbergh 2016). Separation of graphene sheet in 2004 is the prevalent idea and predominated in major part. While some of the previous attempts to separate monolayer materials go back well before 2004, it would be unreasonable to ignore them. Only the work of Novoselov and associates was able to effectively convey the exfoliation of a few graphene layers and display its physical properties (Geim and Novoselov 2007). The discovery proved to be a turning point in significant studies including physics, material science, and why are these 2D materials so fascinating? Since it encompasses a wide variety of materials with a wide range of characteristics, the term "2D materials" is typically quite confusing. Two-dimensional materials (or 2D materials) are crystalline solids that have a thickness of a few nanometers or less. These materials include insulators, layered metals, semi-metals, small and intermediate bandgap semiconductors, and layered materials such as black phosphorus (BP). These materials possess exceptional elastic properties, including strength, stiffness, and flexibility. They can be mechanically removed in one or more layers from a substrate. Synthetic two-dimensional materials, including tellurene, germanene, silicene, and several borophenes polymorphs, can be synthesized from precursors in a bottom-up approach.

This research aims to examine the distinct physical and mechanical properties of two-dimensional materials. Specifically, we will focus on the huge surface area, high surface to volume ratio, unique electrical properties, and high mechanical properties, such as stiffness and flexibility. This research paper's primary focus is on 2D materials using density function theory and non-equilibrium Green's function. In order to develop electrodes for rechargeable batteries, gas sensors, and nanoscale electronic devices, this paper investigates the electrical structure and transport properties of projected and synthesized 2D materials. It investigates both vertical and lateral heterostructures in nanoscale devices, including the twisted bilayer black phosphorus nano junction and the graphene/hBN heterostructure Nano gap. The structural, electrical, and transport properties of borophenes, a recently discovered polymorph of 2D borons, are also investigated in this work. The application of these materials to



Vol. 3 No. 4 (April) (2025)

energy storage is included in the paper as well.

Background

Many distinct two-dimensional (2D) systems offer an abundance of unconventional physical properties that can be investigated with methods such as second-harmonic generation (Khan, Zhang et al. 2022), optical contrast, photoluminescence spectroscopy, Rayleigh scattering (Harvey, Backes et al. 2018), Raman spectroscopy (Liang, Xu et al. 2018), and others. To provide a detailed explanation of the previously described commonly utilized optical spectroscopic techniques, some representative instances of 2DMs are provided. This chapter's techniques can be used with a variety of 2D systems, providing new perspectives on their optical and electrical properties. Two-dimensional materials (2DMs) with covalent bonds for atoms within rigid layers and van der Waals interactions for interlayer coupling are widely used in optoelectronics, nano electronics, and photovoltaics, among other research fields, because of their unique optical properties that can be altered by their interlayer coupling, number of layers, stacking order, and even the assemblies in related van der Waals heterostructures (vdWHs). Optical spectroscopy is widely used to study physical properties resulting from light-matter interaction, including electronic band structure, lattice vibrations, electron-phonon coupling, etc. This chapter summarizes the various 2DMs and related vdWH before focusing on recent advancements in optical spectroscopic research on 2DMs.

Chemical doping can be used to inorganically functionalize two-dimensional materials by substituting a small number of the original material's atoms with new ones. Early investigations focused on the nitrogen substitution in graphene. Examples of how inorganic elements can chemically dope 2D materials. There is a report on the first STM image of nitrogen-doped graphene (Joucken, Tison et al. 2012). Subsequently released studies that revealed the nitrogen doping on graphene's atomic structure. While the two works show nitrogen-doped graphene with triangular patterns in their STM images, they use different methods to replace the nitrogen. The majority of the nitrogen dopants from the study are added during the CVD growth of graphene on copper foil by mixing CH₄, H₂, and NH₃ as precursors (Lee, Bae et al. 2019).

(Joucken, Tison et al. 2012) add the nitrogen atoms by means of a nitrogen plasma on graphene generated on SiC (0001) substrate in a UHV cell. The central nitrogen atom is surrounded in a triangle shape by three carbon atoms. Initial theoretical research based on the (Maddox IV 2012). According to additional study, tip bias has no effect on the various STM morphologies that have been seen; instead, tip-sample distance, tip composition, and tip shape do. In contrast, (Zhao, He et al. 2011). The position of the Dirac point with respect to the Fermi level can be read from the STS spectra. However, because to the inelastic tunneling between the tip and the graphene, the Dirac point measurement may not be very accurate. By breaking the graphene surface's symmetry and forming an elastic tunneling channel, the nitrogen dopant drastically (around 500 times) increases the conductance close to the Fermi level. (Zhao, Levendorf et al. 2013) reported on an STM study of boron dopants on graphene. Similar doping methods, such as the combination of CH₄, H₂, and B₂H₆, are used in the CVD procedure for the development of graphene on copper foil, shows the boron dopant's STM image on graphene. In addition to changing the material's



Vol. 3 No. 4 (April) (2025)

electrical properties, transition metal atomic substitution has been demonstrated to induce magnetic moments in graphene both theoretically and physically (Sethulakshmi, Mishra et al. 2019). (Robertson and Robertson 2013) showed that ion irradiation produces single carbon vacancies on monolayer epitaxial graphene.

Several 2D materials have been introduced in this chapter, such as metal oxide nanosheets, phosphorene, BNNSs, TMDCs, graphene, and silicene. Heterostructure 2D materials, which combine the aforementioned 2D materials with different physical properties, have also been investigated as a way to improve the characteristics of single-phase 2D materials (Li, Qian et al. 2021) (Fig. 1.1). Because each individual 2D material has a unique structure and set of physical properties, it is expected that the heterostructure 2D materials will exhibit synergistic optoelectronic capabilities that are distinct from those of regular bulk material.

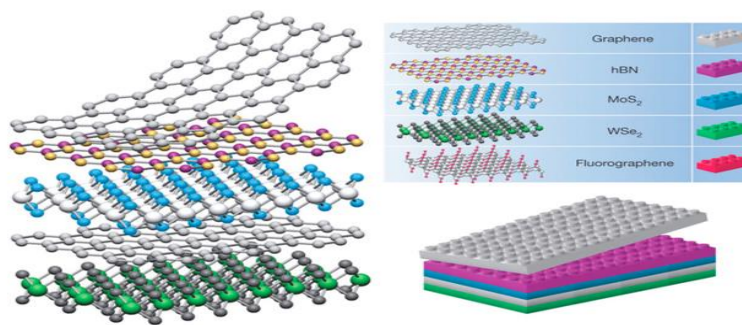


Figure 1: Aforementioned 2D materials with various physical properties(diagram)

One kind of 2D heterostructure is graphene on BNNSs. Dean et al. have built graphene devices on BNNSs via direct mechanical assembly [84]. The graphene layer is added to the BNNS after being deposited on a sacrificial film. By eliminating the sacrificial layer, heterostructure graphene/BNNS sheets with an ultra-high mobility of $106 \text{ cm}^2/\text{V s}$ are produced. BNNSs not only serve as graphene's substrate but also envelop the material in a protective shell. When exposed to air, the graphene devices with BNNS protection do not deteriorate. Multilayer heterostructures with graphene and BNNS have been reported. Additionally, field-effect tunneling transistors can be made using graphene and BNNS or graphene and TMDC heterostructures. Several 2D materials have been previously offered as viable Si alternatives in solar cells due to their compatibility with devices lower than micron dimensions. Solar cells made of heterostructure 2D materials have only recently been reported. After being adjusted for chemical doping and electrical gating, the $\text{MoS}_2/\text{h-BN}/\text{GaAs}$ heterostructure's power conversion efficiency (PCE) was 9.03%. The open-circuit voltage increased and the maximum PCE was 10.93% when BNNSs were inserted between graphene and Si as layers that blocked electrons and transported holes.

Density Function Theory

In this chapter, we elucidate the theoretical underpinnings of the DFT and the computational methodology employed in the electronic structure and transport



Vol. 3 No. 4 (April) (2025)

calculations presented in the thesis. This paper also includes a brief description of how the DFT is used in atomic scale computations for the electrical structure calculations. This allows one to comprehend the structural and electrical properties of materials, particularly 2D materials like graphene and other 2D crystals. This is a synopsis of the DFT analysis of 2D materials. Representing the total energy of a system as a function of electronic density is the main idea. The aim is to find the electronic density in DFT that minimizes this energy functional. The electronic structure can only be computed by solving the Kohn-Sham equations, a set of equations derived from DFT. The electronic wave functions and eigenvalues of the material are obtained from these equations, providing information on its electronic structure. DFT approximates the exchange-correlation energy, which accounts for the many-body interactions among electrons. To achieve exact results, it is imperative to identify the appropriate functional. To reduce the computing burden of DFT calculations, pseudopotentials are often employed. Phonon calculations, which are required to understand the vibrational properties of 2D materials, can be performed using DFT. The results of these calculations include information on the phonon dispersion, vibrational modes, and thermal properties. Using DFT, scientists examine the optical properties, charge distribution, electronic band structures, bandgaps, electronic density of states (DOS), and work functions of 2D materials. These attributes provide insight into the material's behavior and its applications. Thanks to the density functional theory (DFT)-based first-principles approach, the atomistic structure of black phosphorus for SIBs and the interaction between Li and the silicon (Si) electrode are better understood at the atomic level.

Recently, a first-principles analysis has been conducted on two-dimensional (2D) materials, such as niobium diselenide, phosphorene and graphene heterostructures, transition metal dichalcogenide nanotubes, and phosphorene as potential anode materials for batteries (Ladha 2019). The focus of the current study is on an overview of the DFT-based first-principles parameters that are used to evaluate the metal-ion battery electrode materials. Examined were metal-ion battery electrodes composed of 2D materials, including metal dichalcogenides, metal carbides, graphene, phosphorene, and borophene. It was thought that the characteristics of the electrode materials were determined by their atomic level structure. Graphene is a single sheet composed of closely spaced carbon atoms arranged in a two-dimensional honeycomb structure. In a single-layer graphene, carbon atoms are connected to sp^2 hybridized carbon atoms to form a benzene ring, with each atom contributing an unpaired electron. Graphene can also form nanoribbons and nanotubes. Furthermore, (Wang, Zhang et al. 2017) created an electrode consisting of reduced graphene oxide (r-GO) and tin oxide (SnO_2). It was folded and resembled paper.

Hohenburg- Kohn Theorem

It was invented independently by Pierre Hohenberg and Walter Kohn in 1964. The theorem is the basis of density functional theory (DFT), a powerful computational method for examining the electrical structure of atoms, molecules, and solids. This theory allows scientists to minimize the total energy in relation to the electron density, which allows them to calculate a system's electronic properties. The Hohenberg-Kohn theorem, which states that the energy of the ground electronic state is a specific function of the electron density,



Vol. 3 No. 4 (April) (2025)

is the foundation of density functional theory. This property, together with a related vibrational theorem, encouraged the development of useful empirical representations of the density functional, which yield reliable electronic energy estimations even for complex chemical systems. Hohenberg-Kohn theorem: shown that the one-particle reduced density matrix (1RDM) has a universal functional, which is a nondegenerate ground-state N -particle wave function. Gilbert extended this theorem in 1975 to include nonlocal external potentials. A straightforward prescription is possible by representing the ground-state energy as an exact functional of the ground-state two-particle reduced density matrix (2RDM). The functional N -representability problem arises, however, when approximation 2RDMs in terms of the 1RDM produce energy functionals that remain reliant on the 2RDM. The majority of approximation functionals in use today are not N -representable due to Coleman's N -representability criteria on the 1RDM being insufficient to ensure that the reconstructed 2RDM is N -representable. The majority of approximation functionals in use today are not N -representable due to Coleman's N -representability criteria on the 1RDM being insufficient to ensure that the reconstructed 2RDM is N -representable.

The majority of approximation functionals in use today are not N -representable due to Coleman's N -representability criteria on the 1RDM being insufficient to ensure that the reconstructed 2RDM is N -representable. Recent advances in understanding and the development of functionals have been made possible by the systematic method for deriving pure-state N -representability criteria for the 1RDM.

The 1RDM is expressed in terms of the natural orbitals (NOs) and their occupancy numbers (ONs) using the spectral decomposition in most applications. The reconstruction of the 2RDM is based on the PNOFi family of functionals under the requisite ensemble N -representability constraints. The resultant ONs satisfy the prerequisites for pure-state N -representability conditions to hold, allowing for the construction of vibrational Euler equations for energy minimization. The ground state of every many-particle system interacting with a fixed antiparticle interaction is a particular functional of the electron density $n(\mathbf{r})$, as per the first Hohenberg-Kohn theorem (Hohenberg and Kohn, 1964). This implies that the ground-state wave function may be expressed as a specific functional of the ground-state electron density, $\psi = \psi(n)$, by reversing equation. As a result, the ground-state density can be used to describe the ground-state energy E . Hohenberg-Kohn theorem consists of two theorems.

Theorem 1

The ground state density, $n_0(\mathbf{r})$, determines the potential $V_{\text{ext}}(\mathbf{r})$ uniquely, up to a constant, for any system of interacting particles in an external potential $V_{\text{ext}}(\mathbf{r})$. The first theorem only provides the presence of an electron density functional as the fundamental variable; its precise shape is unknown. The functional attribute is defined by the second theorem.

Theorem 2

Any external potential V_{ext} can be used to derive the universal functional for the energy $E[n]$ in terms of density $n(\mathbf{r})$. The global minimal of the energy functional for a given V_{ext} is the system's ground state energy, and the ground state density $n_0(\mathbf{r})$ is the exact density that minimizes the functional. Since a heuristic proof



Vol. 3 No. 4 (April) (2025)

of these theorems can be found in DFT textbooks [102–104], we will not be providing one here. When these two theorems are combined, the energy functional can be expressed as

$$E_{HK}[n] = F_{HK}[n] + \int d^3r V_{ext}(r)n(r).$$

All internal energies, including kinetic and potential energies, are defined by F_{HK} in this instance. One way to express the total internal energy functional is as

$$F_{HK}[n] = T[n] + E_{int}[n].$$

The external potential has no bearing on the previously mentioned equation; the density is the only variable that matters. Therefore, the design of this function needs to be universal. The global minimum of the functional is the exact ground state total energy of the system, or E_0 . The exact ground state density, or $n_0(r)$, is the particle density that minimizes this functional. The variation AL method can be used to calculate the ground state density. They do not, however, offer any recommendations for the construction of the functional that yields the ground state energy. In addition, Kohn-Sham developed the concept of a non-interacting reference system built from a set of orbitals in their formalism to enable highly accurate calculations of the majority of the kinetic energy (Pitts 2021).

Applications

The understanding of the possibilities of 2D materials is greatly advanced by our research into their photocatalytic and photovoltaic activities. We have found the potential novel materials that improve the efficiency of environmental cleanup systems and solar energy devices by investigating their distinct features. These revelations advance our understanding of how to optimize 2D materials for greater effectiveness in these kinds of applications. There are significant practical benefits to this research. Improved 2D materials' photocatalytic capabilities may result in more efficient pollution management and cutting-edge approaches to environmental remediation. Similar to this, enhancements in the photovoltaic characteristics of 2D materials may increase solar cell efficiency and aid in the creation of more environmentally friendly energy sources. Furthermore, the utilization of superior materials can result in cost savings, which could increase the accessibility and economic viability of these technologies. Furthermore, our results provide opportunities for more investigation and application. The findings may open the door to the investigation of other two-dimensional materials and their uses, leading to further advancements in the field. These developments could result in new goods and technology that more successfully handle energy and environmental issues in the real world.

Aims and Objectives

The current project has the following goals and objectives:

1. To investigate the photovoltaic and photocatalytic characteristics of 2D materials.
2. To look into the band structure of electronics.
3. To examine 2D materials' optical characteristics.

Literature Review



Vol. 3 No. 4 (April) (2025)

Synthesis of titanium oxide

By watching bubbles emerge from a titanium dioxide electrode in 1967, Professor Fujishima made the discovery of titanium dioxide's effects (Hashimoto, Irie et al. 2005). The presence of hydrogen and oxygen gas in these bubbles led to the discovery of the Honda-Fujishima phenomenon, or photocatalysis, on the surface of titanium dioxide. Since then, air filtration and antibacterial systems have made advantage of this discovery. In 1989, he tried painting titanium dioxide thin film on the walls and ceiling of a hospital operating room. As a result, there was less bacterial contamination in that room (Fujishima and Zhang 2006). Because of its inexpensive cost, non-toxicity, photostability, and biocompatibility, TiO_2 is a potential material in photocatalysis (Dal Santo and Naldoni 2019). There are two primary approaches for creating nanoparticles (NPs): top-down and bottom-up. In bottom-up synthesis, individual nanoparticles are placed after chemical synthesis and self-assembly (Ostiguy, Lapointe et al. 2006), whereas in top-down synthesis, atoms or molecules are shrunk to nanometric dimensions (Maynard and Aitken 2007). TiO_2 nanocrystal nucleation and agglomeration are influenced by the sintering temperature and pH level, according to Hu and colleagues (Hu, Tsai et al. 2003).

Ball milling is a specialized technique used in top-down synthesis together with laser ablation, etching, sputtering, and grinding. NMs find application in diverse areas such as paint (Chen, Koh et al. 2022), cosmetics (Fytianos, Rahdar et al. 2020), polymer coating, and catalysts (Sharma, Ojha et al. 2015). Controlling the size and shape of NPs depends on variables like monodispersed, pH regulation, and doping the titania surface. The activity of Mo^{6+} -doped TiO_2 rises by a factor of two when compared to pure TiO_2 , and 1% is the optimal concentration for NPs (Zhang, Wu et al. 2014). Adán and associates observed significant variations in the surfaces, anatase, and rutile contents of TiO_2 particles (Adán, Bahamonde et al. 2007).

Sole Gel Methods of TiO_2

The transmission and separation of the photo-generated electrons and holes were facilitated by the titania particles' monodispersity, which was created using the sol-gel synthesis process (Shkrob and Sauer 2004). Second, because the surface of titania modifies the charge compensation depending on the pH of the system, pH management is an additional important consideration (Raza 2017). Thirdly, for many applications, doping the titania surface is essential. Fourth, another parameter that may be used to change the shape and size of NPs is the calcination temperature (Juliet, Ramalingom et al. 2017).

Role of Temperature and pH on TiO_2 Synthesis

Differentiating the drying methods and calcination temperatures of nano-sized TiO_2 has significant influence on its crystal structure, energy band structure, optical adsorption property, surface quality, and photocatalytic activity (Lal, Sharma et al. 2021). Ani and associates elucidated the effects of temperature, precursor concentration, and the molar ratio of $\text{H}_2\text{O}/\text{TiCl}_4$ on phase composition and particle size (Ani, Savithri et al. 2005). In a different experiment, Xu and colleagues produced sol-gel-mediated anatase titania powder using both sol-gel and thermal techniques (Rathore, Kulshreshtha et al. 2020). They verified that the anatase phase endures and is predominant



Vol. 3 No. 4 (April) (2025)

throughout the 400–510 °C calcination temperature range, and that the temperature at which anatase converts to rutile is 510 °C. Phosphors hindered the formation of anatase and rutile crystallites, resulting in smaller crystallite sizes. Rutile generation was highest in potassium-rich TiO₂ and lithium-supplied TiO₂, while anatase and rutile crystallite size remained unaffected. Temperature-dependent phase control of TiO₂ nanoparticles is supported, requiring further investigation (Dubey 2018). Isley and Penn discovered that adding HCl during the manufacturing process increased the amount of amorphous TiO₂ in contrast to HNO₃ in the sol gel synthesis of TiO₂ at pH 3 (Isley and Penn 2006). Sol-gel mediated TiO₂ samples were produced by Adan and colleagues at various pH values and heat treatments (Ibrahim 2015).

Control of Crystallite Size in TiO₂ Synthesis

Particle size is a critical feature that continuously draws attention to the detrimental properties of nanoparticles. Size and shape have a major impact on the physicochemical properties of metallic nanoparticles (Cuenya 2010). TiO₂ films showed size-dependent photodegradation of methylene blue (MB) solution at the nanoscale, according to Chen and colleagues (Chen, Liu et al. 2013). They looked at the effects of particle size on seeding and photocatalysis. Chen and associates looked at the connection between NPs' photocatalytic activity and particle form. Garvie studied the dependence of particle size on phase transitions. According to him, the relative stability of a system is also influenced by the grain size (Garvie and Goss 1986).

TiO₂ mobility in different porous media

Understanding the behavior and transport of nanoparticles (NMs) in complex aqueous matrices is crucial for commercial production and usage. Factors such as interactions between NPs (Foroozesh and Kumar 2020), porous mediums, suspended colloids, organic and inorganic constituents, pH, and electrolyte concentration influence their mobility in environmental contexts. The chemistry of the medium significantly influences NMs' ultimate fate, with higher sticking efficiency leading to more aggregation. Chowdhury and colleagues conducted a series of experiments to gain a better understanding of the effects of chemistry, NP concentration, and hydrodynamic properties on TiO₂ NP mobility and retention over sandy porous media (Chowdhury, Hong et al. 2011).

Method of Calculation

To ascertain the physical and chemical characteristics of any given material, the atomic nucleus and electrons are essential components. Electronic composition affects microscopic and atomic features like as optics, magnetic properties, and crystallization. Investigating the electric composition thereby appeals to the material's observation, particularly the physics and chemistry sections. Solving the electric structure would not be easy because the electrical interlink-age in nature is quantum persistent and challenging to express because of the growing electron strength. This limitation applies to many body physics, which is a field of study within physics.

The Many-Body Problem

An example of the many-body technique is the wave function $\Psi(\{\vec{r}_i, \vec{R}_\alpha\}, t)$, for



Vol. 3 No. 4 (April) (2025)

each electron, which is usually dependent on both time and position. The non-relativity of the system is governed by Schrödinger equality, which is:

$$\Psi(\{\vec{r}_i, \vec{R}_\alpha\}, t), \quad (3.1)$$

The operator of total energy, which has a linked nucleus and electrons and uses the many-particle interrelating technique (Chaudhuri and Chattopadhyay 2017), is represented by this Hamiltonian.

$$\hat{H} = -\frac{\hbar^2}{2m_e} \sum_i \nabla_i^2 - \sum_i \frac{\hbar^2}{2M_\alpha} \nabla_\alpha^2 - \sum_i \sum_\alpha \frac{Z_\alpha e^2}{|\vec{r}_i - \vec{R}_\alpha|} + \sum_i \sum_{j>i} \frac{e^2}{|\vec{r}_i - \vec{R}_j|} + \sum_\alpha \sum_{\beta>\alpha} \frac{Z_\alpha Z_\beta e^2}{|\vec{r}_\alpha - \vec{R}_\beta|} \quad (3.2)$$

The provided Hamiltonian lacks a time-dependent expression (Kerman and Koonin 1976). As a result, the wave function could only be understood as the outcome of an equation that depended on both time and space.

$$\Psi(\{\vec{r}_i, \vec{R}_\alpha\}, t) = \varphi_E(\{\vec{r}_i, \vec{R}_\alpha\}) e^{-iEt} \quad (3.3)$$

$$\hat{H}\Psi = E\Psi \quad (3.4)$$

All kinds of systems needed to incorporate estimation in order to employ Schrödinger's equation. The fundamental estimation shows that the mobility of the electron is much greater than that of the nuclei since the electron is lighter by a factor of 103. It is therefore expected that the electron will rapidly acquire the nucleus's direct site at this position. The Born-Oppenheimer approximation is the dissociation or breaking of this wave function (Butler 1998).

$$\hat{H} = -\frac{\hbar^2}{2m_e} \sum_i \nabla_i^2 - \sum_i \sum_\alpha \frac{Z_\alpha e^2}{|\vec{r}_i - \vec{R}_\alpha|} + \sum_i \sum_{j>i} \frac{e^2}{|\vec{r}_i - \vec{R}_j|} \quad (3.1)$$

The Ewald's process uses the nucleus-nucleus connection, the last expression of the 3.2 equation, to approximate the total energy of the system. The aforementioned reasons make solving Schrödinger's equation difficult, even when the previous estimation is taken into consideration.

- To measure the wave capability of the many-body framework, a sum of 4N variables is needed, as there are approximately 1023 electrons.
- Due to the fact that solids contain electrons, which affect electron mobility via the relationship (electron) term, the second component of the condition.

Hartree created the first technique ever to tackle the aforementioned issue by considering the many-electron wave function as a result of the single-electron wave functions. One may estimate the single particle Hamiltonian (Hartree) equations using the variational technique (Hylleraas 1964). The resulting equations are the same as the Schrödinger equation with the addition of a "Hartree" potential term. Nevertheless, nothing is known about the fermionic



Vol. 3 No. 4 (April) (2025)

wavefunction's characteristics(Kohn 1999).

The aforementioned formalisms are based on the wave function of the many-body electrons(Nishijima 1954). It is therefore expected that for bigger size systems, they will be much more computationally expensive. The wave function cannot be measured empirically due to its complexity. There are $4N$ variables for every N electron: 3 spatial and 1 spin variables. The degree of freedom has been reduced by the electron density (if used as a variable), which can significantly reduce computation time. The goal of Density Functional Theory (DFT), widely recognized as the most widely applied and adaptable approach in modern condensed matter computing, was to solve Schrödinger's equation for many-body systems where the electron density was the variable.

Kohn-Sham Scheme

By getting them back acquainted with either a fictitious system traveling in a sufficient and efficient V_{eff} non-interacting electrons. Thomas-method constraints were overcome by Walter Kohn and his pupil Sham, with the exception of a small portion of the total that is determined by an assumed functional in order to achieve the same electron density in both interacting and non-interacting systems, Fermi's effective potential needs to be set to an exact value; this model captures this fact as well as possible.

Schrodinger wave equation (SWE) is:

$$H\psi_i(x_1, x_2, \dots, x_n) = E_i\psi_i(x_1, x_2, \dots, x_n) \quad (3.6)$$

The equation to get the total lowest state energy of interacting inhomogeneous electrons uses the static potential $V(r)$.

$$E[\rho] = V[\rho] = U[\rho] + G[\rho] \quad (3.7)$$

The following is Kohn Sham's explanation of total energy partitioning:

$$E[\rho] = T_s[\rho] + V[\rho] + U[\rho] + E_{xc}[\rho] \quad (3.8)$$

The left-hand term, kinetic energy, is a system to make function and an implicit density function. The K . E of non-interacting particles is the average of the K . E s of the individual particles.

$$T_s[\rho] = \frac{-\hbar^2}{2m} \sum_i^N \int \phi_i^*(r) \nabla^2 \phi_i(r) d^3r = T[\{\phi_i(\rho)\}] \quad (3.9)$$

The second part, which stands for the classical electron interaction and the coulomb energy, can be expressed as follows:

$$U = \frac{q^2}{2} \int \frac{\rho(r)\rho(r')}{|r-r'|} drdr' \quad (3.10)$$

The nuclei's external potential, represented by

$$V[\rho] = \int v(r)\rho(r)dr \quad (3.11)$$



Vol. 3 No. 4 (April) (2025)

An arbitrary could exist for a density that varies slowly enough, but it doesn't seem to have a specific definition.

$$E_{sc}[\rho] = \int \rho(r)\epsilon_{xc}(\rho(r))dr \quad (3.12)$$

The correlation function and per-electron energy of exchange of a homogeneous electron plasma with density r are derived here. Exchange-correlation energy is produced when the correlation and exchange energies combine.

$$E_{XC} = E_X(\rho)_{\text{exchange}} + E_c(\rho)_{\text{correlation}} \quad (3.13)$$

$$E_x[\rho] = \int \rho(r)\epsilon_x(\rho(r))dr \quad (3.14)$$

The interaction potential provides the exchange energy and explains the reduction of energy because of anti-symmetry. The orbital of a single particle serves as one foundation for this claim.

$$\epsilon_x[\{\phi_i(\rho)\}] = -\frac{q^2}{2} \sum_{j,k} \int d^3r \int d^3r' \frac{\phi_j^*(r)\phi_k^*(r')\phi_j(r')\phi_k(r)}{|r-r'|} \quad (3.15)$$

The energy of exchange molecules "a" at point "r" and "b" at point "r" is described in a single sentence. The additional energy savings in a real system come from the mutual avoidance of interacting electrons, which happens when electrons with opposite spins try to control their locations to conserve energy.

$$\epsilon_c = \sum_{j<k} \frac{q^2}{|r-r'|} = \frac{q^2}{2} \int d^3r \int d^3r' \frac{\rho(r)\rho(r') - \rho(r)\delta(r-r')}{|r-r'|} \quad (3.16)$$

The Kohn Sham equation states that E must minimize with respect to density in order to obtain ground state energy.

$$0 = \frac{\delta E[\rho]}{\delta \rho(r)} = \frac{\delta T_s[\rho]}{\delta \rho(r)} + \frac{\delta U[\rho]}{\delta \rho(r)} + \frac{\delta V[\rho]}{\delta \rho(r)} + \frac{\delta T_{XC}[\rho]}{\delta \rho(r)} \quad (3.17)$$

$$= \frac{\delta T_s[\rho]}{\delta \rho(r)} + v(r) + V_c(r) + V_{xc}(r) \quad (3.18)$$

In some cases, it is impossible to reduce a dense non-interacting system.

$$0 = \frac{\delta E_s[\rho]}{\delta \rho_s(r)} = \frac{\delta T_s[\rho]}{\delta \rho_s(r)} + \frac{\delta V_s[\rho]}{\delta \rho_s(r)} + \frac{\delta T_{XC}[\rho]}{\delta \rho(r)} = \frac{\delta T_s[\rho]}{\delta \rho(r)} + V_s(r) \quad (3.19)$$

analyzing the aforementioned two equations.

$$v_s(r) = V(r) + V_c(r) + V_{xc}(r) \quad (3.20)$$

It can be assumed that the outcome of both minimizations is the same. If

$$\rho_s(r) = \rho(r) \quad (3.21)$$

Consequently, a density over several body systems in either possibility may be evaluated by changing the values for a single body system in one potential, which



Vol. 3 No. 4 (April) (2025)

is represented as.

$$\left[\frac{-\hbar^2}{2m} \nabla^2 + v_s(r) \right] \phi_i(r) = E_i \phi_i(r) \quad (3.22)$$

It releases the orbital that represents the original system density through the following connections:

$$\rho(r) = \rho_s(r) = \sum_i^N f_i |\phi_i(r)|^2 \quad (3.23)$$

Naturally, the solution to non-interacting problems takes the role of the minimization problem.

3.4 The Exchange Correlation Potential:

The KS equations, despite certain imperfections (Baer, Neuhauser et al. 2013). The density functional for a specific SWE is all that the HK 1st theorem offers; it says nothing about the real functional. The second theorem gives the density at which the lowest energy functional appears to imply ground state features, but it does not describe the exact functional (Jones 2015). The components will be briefly explained after the accurate ground state energy has been obtained.

$$E[\{\psi_i\}] = E_{\text{known}}[\{\psi_i\}] + E_{X-C}[\{\psi_i\}] \quad (3.2)$$

It is concluded that E_{X-C} is known $[\phi]$, that consists of three coulomb interaction choices with a single electronic K.E term—n-n, e-e, and e-n—is present in the composite functional. The exchange-correlation everything's functional form is defined by the second term, $E_{X-C}[\phi]$.

$$\left[-\frac{\hbar^2}{2m} \nabla^2 + V_H(r) + V_{X-C}(r) + V(r) \right] \psi_i(r) = \epsilon_i \psi_i(r) \quad (3.3)$$

This can be used to characterize $V(r)$, which stands for interactions.

$$V_{X-C}(r) = \frac{\delta E_{X-C}(r)}{\delta \rho(r)} \quad (3.4)$$

Because of the uncertainty around the XC-practicality, many mBJ, GGA, and LDA counterparts are used.

Local Density Approximation (LDA)

The exchange correlation energy E_{xc} is now the most often used method for calculating local density approximation, also known as local spin density approximation (Ortenzi, Mazin et al. 2012).

Similarly, the LSDA

$$E_{XC}^{LDA}(\rho_{\uparrow}(r), \rho_{\downarrow}(r)) = \int \rho(\vec{r}) \epsilon_{xc}(\rho_{\uparrow}(\vec{r}), \rho_{\downarrow}(\vec{r})) d\vec{r} \quad (3.5)$$

$\rho(\vec{r}) \epsilon_{XC}$ is a local density function in LDA. Correlation and trade make up these two areas.

In the 1920s, Fermi and Thomas calculated the exchange densities of an electron gas with non-interacting homogeneity (Bene and Nagy). Dirac employed the ideas of Fermi and Thomas to compute an exchange fraction energy.



Vol. 3 No. 4 (April) (2025)

$$\epsilon_c(\rho(\vec{r})) = -\frac{3}{4} \sqrt{\frac{3\rho(\vec{r})}{\pi}} \quad (3.6)$$

High accuracy quantification of the association and additional data can be obtained by Monte Carlo simulations (Bystrov, Naboka-Krell et al. 2024).

Generalized Gradient Approximation (GGA)

Because it reduces computational effort and eliminates some of the conflicts in the LDA, generalized gradient approximation, or GGA, is preferable to LDA (Zhang, Sun et al. 2017).

Furthermore gradient $\nabla(\rho(\vec{r}))$

$$E_{XC}^{GGA}(\rho(\vec{r})) = \int \rho(\vec{r}) \nabla \rho(\vec{r}) \epsilon_{XC}(\rho(\vec{r})) d\vec{r} \quad (3.7)$$

GGA significantly improves ground state properties of molecules, light atoms, and solids, including ground state energies, bond lengths, and dissociation energies (Livshits and Baer 2007). Perdew, Burke, and Ernzerhof created a modified GGA (PBE) to fit the physical and mathematical requirements of DFT (Xu and Goddard III 2004), but it fails to calculate thermo-chemical or total atomic energies. Handy and co-workers experimented with 93 chemical processes, stating that PBE fails these criteria. Goddard and Xu introduced xPBE, which functions similarly to PBE, but is less accurate in solids and atoms. FX exchange rising component is present in many systems, suggesting arbitrary precision. Recreating GGA, which is slightly more accurate than PBE, in these atoms and solids would be expensive.

Augmented Plane Wave (APW)

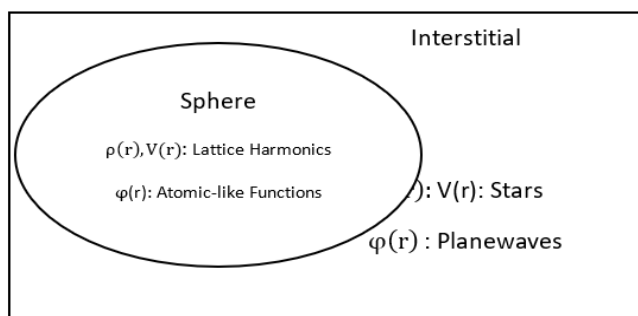
The APW method separates the unit cell into two parts:

- A "Muffin-Tin" sphere is a sphere that can be orientated toward each of its component nuclei.
- The remainder of any unit group is referred to as the interstitial area as seen in Figure 2.

Linearized Augmented Plane Wave

The difficulties faced by APW are addressed by the LAPW method. When muffin-tin (MT) is introduced about each atom, an LAPW notion consists of many parts.

$$V(r) = \left\{ \frac{\sum_{lm} V_{lm}(r) Y_{lm}(\hat{r})}{\sum_K V_K e^{iKr}} \right\} \quad (3.8)$$





Vol. 3 No. 4 (April) (2025)

Figure2: APW scheme for unit cell division

Full-Potential Linearized Augmented Plane Wave technique

The efficiency of a material with no form approximation (FP-LAPW) is defined using full potential linearized augmented plane wave approximation (Chowdhury, Rigosi et al. 2022).

$$\psi(\vec{r}) = \left\{ \begin{array}{l} \sum_{LM} V_{LM}(\vec{r}) Y_{LM}(\vec{r}) \dots \dots (i) \\ \sum_K V_K \exp(i\vec{k} \cdot \vec{r}) \dots \dots (ii) \end{array} \right\} \quad (3.9)$$

In this case, equation (i) represents the atomic sphere's inside, and equation (ii) represents its outside.

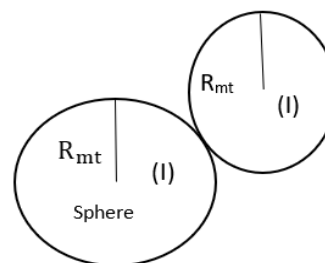


Figure 2: FP-LAPW scheme for unit cell division

The WIEN2K Program

The programming tool WIEN2K was utilized to do the calculations in this study (Schwarz 2003).

WIEN2K uses a satisfactory combination basis functional containing the atomic and PW functions to determine the values with high precision (Schwarz, Blaha et al. 2010).

Basic Step for simulation in WIEN2K

Structure generate

- Store the downloaded CIF file in the designated folder.
- Choosing information from a single group of spaces
- The material's geometry. • RMT atomic characteristics are obtained by unit cell implementations.

Initialization

- K-point gathering over the first Brillion zone.
- Recognition of lattices.
- Generation of intelligent data.

Presentation of code Wien2K

The Wien2K in DFT is used to employ LAPW to determine the crystal structure of an atom (Cottenier 2002). A range of fundamental broods within the atom are used in WIEN2K by chemically significant metals, while LAPW is utilized for other types. Among the applications are:

Structural optimization

Since the power in question is expressed in the WEIN2 K language, it is not especially susceptible to this tactic. In a similar way, the power function of the energy volume increases with the muffin tin radius (RMT) of the particles. The fusion of this set is controlled by the cutoff value $RMT K_{max} = 6-9$, where RMT



Vol. 3 No. 4 (April) (2025)

is the tiny atomic sphere radius and K_{max} is the largest magnitude of K . A wave that is close to the nucleus goes away from the nucleus even when very little muffin tin rises.

Band structures and Density of states (DOS)

The network power loss could be computed using the power band and the regional value. The electron entropy is large by active entropy. The Fourier transform should be used to calculate the static structure characteristic [60]. This can also be used to find other qualities, such as optical, electrical, mechanical, etc. The WIEN2K technique is used to calculate the band structure. To access the electronic structure of the substance, a comprehensive procedure is required.

Thermal structures

Combination structures may be analyzed using the lattice's most important feature, which studies atomic vibrations in relation to its position to do so. WIEN2K can be used to estimate a wide range of structures and uncover information about their numerous properties, including electrical, thermal, optical, and other properties. With supercells, we can dope different substances and change their properties (Schwarz 2003).

Employed method for calculation

To find the KS equations shown in the WIEN2K method, the ab-initio data may be analyzed using the full-potential linearized augmented wave in the DFT (Khireddine 2024). To apply an exchange-correlation advance, PBE-sol is used to capture the primary electrical, optical, magnetic, and optoelectrical properties. RMT has turned into the MT share's least boundary line, according to $RK_{max}=5.0-91$, the wave vector, under which K_{max} is presumably the maximum value of the main vector in the interactional show at a higher.

Expected Results

We expect to find considerable improvements in the photocatalytic effectiveness of the two-dimensional (2D) materials under investigation. In particular, we anticipate that when exposed with both UV and visible light, these 2D materials will perform notably better in the destruction of environmental contaminants. The increased surface area-to-volume ratio of the materials is expected to provide this enhancement since it improves their contact with light and contaminants. Additionally, a key factor in this increased photocatalytic activity is anticipated to be the decreased electron-hole pair recombination rates in 2D materials. We hope to learn more about how the special electrical characteristics of 2D materials, including the band structure and charge carrier factors, contribute to enhanced photocatalytic performance by carefully examining the processes underlying these activities. Our findings indicate that the use of 2D materials in solar devices can lead to a significant improvement in the efficiency of power conversion (PCE) in the field of photovoltaic applications. The expected enhancement is ascribed to various intrinsic characteristics of two-dimensional materials. Initially, it is anticipated that their enhanced capacity to assimilate light across various wavelengths will result in superior light-harvesting capacities. Second, 2D materials' enhanced charge transport capabilities along with elevated charge carrier mobility are anticipated to lower energy losses and



Vol. 3 No. 4 (April) (2025)

boost the effectiveness of charge collection inside the gadget. Additionally, we anticipate that devices made with these 2D materials will be more stable and resilient, demonstrating better resistance to deterioration when exposed to light and outside influences for extended periods of time. Additionally, our research predicts that band gap engineering in 2D materials will be successfully shown. We anticipate being able to customize the optical and electronic characteristics of these materials to maximize their performance in photovoltaic and photocatalytic applications by adjusting the band gap through a variety of techniques, such as alloying or structural alterations. The materials may be tailored for particular light wavelengths and desirable electronic transitions, which is expected to lead to more efficient photocatalytic reactions and improved photovoltaic efficiency.

We also anticipate enhancements in the behavior of charge carriers in the two-dimensional materials. More specifically, we anticipate longer carrier lifetimes and higher charge carrier mobility, which are essential for photocatalytic and photovoltaic applications. Techniques like time-resolved spectroscopy, which will shed light on the actions and recombine rates of charge carriers, are expected to confirm these gains. It is anticipated that improved charge carrier dynamics will result in more effective energy consumption conversion. It is expected that comparative assessments will demonstrate that the 2D materials perform better than traditional materials in a number of important performance criteria. We seek to validate the higher efficiency and potential benefits of 2D materials by comparing their photovoltaic efficiencies and photocatalytic degradation rates to those of traditional materials.

Finally, we hope to find scalable synthesis techniques for the two-dimensional materials while preserving their improved characteristics. Ensuring constant material performance and quality across various production volumes is essential for successful scaling. It is expected that our research will have substantial practical ramifications, with potential applications ranging from renewable energy technology to environmental remediation. Our goal is to open the door for future advancements and applications in photovoltaics and photocatalysis by showcasing the practical advantages and viability of incorporating 2D materials into these domains.

References

- Adán, C., et al. (2007). "Structure and activity of nanosized iron-doped anatase TiO₂ catalysts for phenol photocatalytic degradation." *Applied Catalysis B: Environmental* 72(1-2): 11-17.
- Ani, J. K., et al. (2005). "Characteristics of titania nanoparticles synthesized through low temperature aerosol process." *Aerosol and air quality research* 5(1): 1-13.
- Baer, R., et al. (2013). "Self-averaging stochastic Kohn-Sham density-functional theory." *Physical review letters* 111(10): 106402.
- Bene, E. and A. Nagy "Electron density and correlation energy in density functional theory."
- Butler, L. J. (1998). "Chemical reaction dynamics beyond the Born-Oppenheimer approximation." *Annual review of physical chemistry* 49(1): 125-171.
- Butler, S. Z., et al. (2013). "Progress, challenges, and opportunities in two-dimensional materials beyond graphene." *ACS nano* 7(4): 2898-2926



Vol. 3 No. 4 (April) (2025)

- Bystrov, V., et al. (2024). "Choosing the Number of Topics in LDA Models—A Monte Carlo Comparison of Selection Criteria." *Journal of Machine Learning Research* 25(79): 1-30.
- Chaudhuri, R. K. and S. K. Chattopadhyay (2017). *Many-body methods for atoms and molecules*, CRC Press.
- Chen, M. C., et al. (2022). "Titanium dioxide and other nanomaterials based antimicrobial additives in functional paints and coatings." *Progress in Organic Coatings* 163: 106660.
- Chen, Q., et al. (2013). "TiO₂ nanobelts—effect of calcination temperature on optical, photoelectrochemical and photocatalytic properties." *Electrochimica acta* 111: 284-291.
- Chowdhury, I., et al. (2011). "Mechanisms of TiO₂ nanoparticle transport in porous media: Role of solution chemistry, nanoparticle concentration, and flowrate." *Journal of colloid and interface science* 360(2): 548-555.
- Chowdhury, S., et al. (2022). "Computational methods for charge density waves in 2D materials." *Nanomaterials* 12(3): 504.
- Cottenier, S. (2002). "Density Functional Theory and the family of (L) APW-methods: a step-by-step introduction." *Instituut voor Kern-en Stralingsfysica, KU Leuven, Belgium* 4(0): 41
- Cuenya, B. R. (2010). "Synthesis and catalytic properties of metal nanoparticles: Size, shape, support, composition, and oxidation state effects." *Thin Solid Films* 518(12): 3127-3150.
- Dal Santo, V. and A. Naldoni (2019). *Titanium dioxide photocatalysis*, MDPI.
- Dubey, R. (2018). "Temperature-dependent phase transformation of TiO₂ nanoparticles synthesized by sol-gel method." *Materials Letters* 215: 312-317.
- Fischetti, M. V. and W. G. Vandenberghe (2016). "Mermin-Wagner theorem, flexural modes, and degraded carrier mobility in two-dimensional crystals with broken horizontal mirror symmetry." *Physical Review B* 93(15): 155413.
- Foroozesh, J. and S. Kumar (2020). "Nanoparticles behaviors in porous media: Application to enhanced oil recovery." *Journal of Molecular Liquids* 316: 113876.
- Fujishima, A. and X. Zhang (2006). "Titanium dioxide photocatalysis: present situation and future approaches." *Comptes Rendus Chimie* 9(5-6): 750-760.
- Fytianos, G., et al. (2020). "Nanomaterials in cosmetics: Recent updates." *Nanomaterials* 10(5): 979.
- Garvie, R. and M. Goss (1986). "Intrinsic size dependence of the phase transformation temperature in zirconia microcrystals." *Journal of materials science* 21: 1253-1257.
- Geim, A. K. and K. S. Novoselov (2007). "The rise of graphene." *Nature materials* 6(3): 183-191.
- Harvey, A., et al. (2018). "Non-resonant light scattering in dispersions of 2D nanosheets." *Nature communications* 9(1): 4553.
- Hashimoto, K., et al. (2005). "TiO₂ photocatalysis: a historical overview and future prospects." *Japanese journal of applied physics* 44(12R): 8269.
- Hu, Y., et al. (2003). "Phase transformation of precipitated TiO₂ nanoparticles." *Materials Science and Engineering: A* 344(1-2): 209-214.



Vol. 3 No. 4 (April) (2025)

- Hylleraas, E. A. (1964). The Schrödinger two-electron atomic problem. *Advances in Quantum Chemistry*, Elsevier. 1: 1-33.
- Ibrahim, S. A. (2015). Development of titanium dioxide nanoparticles/nanosolution for photocatalytic activity, Universiti Sains Malaysia.
- Isley, S. L. and R. L. Penn (2006). "Relative brookite and anatase content in sol-Gel-Synthesized titanium dioxide nanoparticles." *The Journal of Physical Chemistry B* 110(31): 15134-15139.
- Jones, R. O. (2015). "Density functional theory: Its origins, rise to prominence, and future." *Reviews of Modern Physics* 87(3): 897-923.
- Joucken, F., et al. (2012). "Localized state and charge transfer in nitrogen-doped graphene." *Physical Review B—Condensed Matter and Materials Physics* 85(16): 161408.
- Juliet, S. S., et al. (2017). "Effect of calcination temperature on titanium oxide nanocrystallites in the anatase phase synthesized by sol-gel route." *IOSR J. Appl. Phys* 9(4): 32-39.
- Kerman, A. K. and S. E. Koonin (1976). "Hamiltonian formulation of time-dependent variational principles for the many-body system." *Annals of Physics* 100(1-2): 332-358.
- Khan, A. R., et al. (2022). "Optical harmonic generation in 2D materials." *Advanced Functional Materials* 32(3): 2105259.
- Khireddine, A. (2024). Ab initio study of physical properties of some solid materials.
- Kohn, W. (1999). "Nobel Lecture: Electronic structure of matter—wave functions and density functionals." *Reviews of Modern Physics* 71(5): 1253.
- Ladha, D. G. (2019). "A review on density functional theory-based study on two-dimensional materials used in batteries." *Materials Today Chemistry* 11: 94-111.
- Lal, M., et al. (2021). "Calcination temperature effect on titanium oxide (TiO₂) nanoparticles synthesis." *Optik* 241: 166934.
- Lee, I., et al. (2019). "Rapid synthesis of graphene by chemical vapor deposition using liquefied petroleum gas as precursor." *Carbon* 145: 462-469.
- Li, W., et al. (2021). "Phase transitions in 2D materials." *Nature Reviews Materials* 6(9): 829-846.
- Liang, F., et al. (2018). "Raman spectroscopy characterization of two-dimensional materials." *Chinese Physics B* 27(3): 037802.
- Livshits, E. and R. Baer (2007). "A well-tempered density functional theory of electrons in molecules." *Physical Chemistry Chemical Physics* 9(23): 2932-2941.
- Maddox IV, W. B. (2012). *Defects and alloying in semiconductors: Computational studies of clusters and surfaces*, Colorado School of Mines.
- Maynard, A. D. and R. J. Aitken (2007). "Assessing exposure to airborne nanomaterials: current abilities and future requirements." *Nanotoxicology* 1(1): 26-41.
- Nishijima, K. (1954). "Many-body Problem in Quantum Field Theory, II." *Progress of Theoretical Physics* 12(3): 279-310.
- Ortenzi, L., et al. (2012). "Accounting for spin fluctuations beyond local spin density approximation in the density functional theory." *Physical Review B—Condensed Matter and Materials Physics* 86(6): 064437.



Vol. 3 No. 4 (April) (2025)

- Ostiguy, C., et al. (2006). "STUDIES AND RESEARCH PROJECTS."
- Pitts, T. (2021). *The Effective Potential in Kohn-Sham Theory*, Durham University.
- Rathore, N., et al. (2020). "Study on morphological, structural and dielectric properties of sol-gel derived TiO₂ nanocrystals annealed at different temperatures." *Physica B: Condensed Matter* 582: 411969.
- Raza, G. (2017). *Titanium dioxide nanomaterials, synthesis, stability and mobility in natural and synthetic porous media*, University of Birmingham.
- Robertson, A. and A. W. Robertson (2013). *Synthesis and characterisation of large area graphene*, Oxford University, UK.
- Schwarz, K. (2003). "DFT calculations of solids with LAPW and WIEN2k." *Journal of Solid State Chemistry* 176(2): 319-328.
- Schwarz, K., et al. (2010). "Electronic structure of solids with WIEN2k." *Molecular Physics* 108(21-23): 3147-3166.
- Sethulakshmi, N., et al. (2019). "Magnetism in two-dimensional materials beyond graphene." *Materials today* 27: 107-122.
- Sharma, N., et al. (2015). "Preparation and catalytic applications of nanomaterials: a review." *Rsc Advances* 5(66): 53381-53403.
- Shkrob, I. A. and M. C. Sauer (2004). "Hole scavenging and photo-stimulated recombination of electron-hole pairs in aqueous TiO₂ nanoparticles." *The Journal of Physical Chemistry B* 108(33): 12497-12511.
- Wang, Q., et al. (2017). "Flexible Two-dimensional Nanomaterials for Lithium-ion Batteries Applications."
- Xu, X. and W. A. Goddard III (2004). "The extended Perdew-Burke-Ernzerhof functional with improved accuracy for thermodynamic and electronic properties of molecular systems." *The Journal of chemical physics* 121(9): 4068-4082.
- Zhang, P., et al. (2014). "Influence of alternating current electric field on the photocatalytic activity of Mo⁶⁺-doped and AgO-loaded nano-TiO₂." *Journal of alloys and compounds* 587: 511-514.
- Zhang, Y., et al. (2017). "Comparative first-principles studies of prototypical ferroelectric materials by LDA, GGA, and SCAN meta-GGA." *Physical Review B* 96(3): 035143.
- Zhao, L., et al. (2011). "Visualizing individual nitrogen dopants in monolayer graphene." *Science* 333(6045): 999-1003.
- Zhao, L., et al. (2013). "Local atomic and electronic structure of boron chemical doping in monolayer graphene." *Nano letters* 13(10): 4659-4665.